Vibrational energy transfer in shock-heated norbornene

John R. Barker
Department of Atmospheric, Oceanic, and Space Sciences, Department of Chemistry, University of Michigan, Ann Arbor, Michigan 48109-2143

Keith D. King
Department of Chemical Engineering, University of Adelaide, 5005 Australia

(Received 25 May 1995; accepted 22 June 1995)

Recently, Kiefer *et al.* [J. H. Kiefer, S. S. Kumaran, and S. Sundaram, J. Chem. Phys. **99**, 3531 (1993)] studied shock-heated norbornene (NB) in krypton bath gas using the laser-schlieren technique and observed vibrational relaxation, unimolecular dissociation (to 1,3-cyclopentadiene and ethylene), and dissociation incubation times. Other workers have obtained an extensive body of high-pressure limit unimolecular reaction rate data at lower temperatures using conventional static and flow reactors. In the present work, we have developed a vibrational energy transfer-unimolecular reaction model based on steady-state RRKM calculations and time-dependent master equation calculations to satisfactorily describe all of the NB data (incubation times, vibrational relaxation times, and unimolecular rate coefficients). The results cover the temperature range from ~300 to 1500 K and the excitation energy range from ~1 000 to 18 000 cm^{-1}. Three different models (based on the exponential step-size distribution) for the average downward energy transferred per collision, $\langle \Delta E \rangle_{down}$ were investigated. The experimental data are too limited to enable the identification of a preferred model and it was not possible to determine whether the average $\langle \Delta E \rangle_{down}$ is temperature dependent. However, all three $\langle \Delta E \rangle_{down}$ models depend linearly on vibrational energy and it is concluded that standard unimolecular reaction rate codes must be revised to include energy-dependent microcanonical energy transfer parameters. The choice of energy transfer model affects the deduced reaction critical energy by more than 2 kcal mol^{-1}, however, which shows the importance of energy transfer in determining thermochemistry from unimolecular reaction fall-off data. It is shown that a single set of Arrhenius parameters gives a good fit of all the low temperature data and the shock-tube data extrapolated to the high pressure limit, obviating the need to invoke a change in reaction mechanism from concerted to diradical for high temperature conditions. Some possible future experiments are suggested.

I. INTRODUCTION

In unimolecular reaction fall-off experiments, the reaction rate coefficient depends both on collisional energy transfer rates and on the energy-dependent microcanonical unimolecular rate coefficient, $k(E)$. Accurate extrapolations of experimental data to the high pressure limit are difficult and it is not easy to separate the contributions of energy transfer from $k(E)$: A clean separation is only possible when additional information is available.

Recently, Kiefer, Kumaran, and Sundaram[1] (KKS) studied shock-heated norbornene (NB) in krypton bath gas and observed vibrational relaxation, unimolecular dissociation, and dissociation incubation times. KKS state that their NB study is the first unambiguous observation of vibrational relaxation and incubation in a molecule larger than a triatomic and only one triatomic has shown unambiguous incubation.[2] Earlier schlieren shock-tube experiments using cyclohexene[3] gave some indication of an incubation time.[4] Usually, only unimolecular fall-off rate coefficients are available, so the additional information provided by this new shock-tube study of NB provides an excellent opportunity to investigate the interplay between vibrational energy transfer and unimolecular reaction over a very wide temperature range. In principle, the three types of data when used together are sufficient to establish a substantially complete model of the shock-induced decomposition process, including the period prior to establishment of steady state.

In this paper, we present a detailed energy transfer-unimolecular reaction model which satisfactorily describes all of the data (vibrational relaxation, incubation, and unimolecular reaction) available for NB. This model is similar in concept to earlier models[4,5] and the NB data make possible the complete analysis. The unimolecular reaction rate data from four different studies of NB cover the temperature range from 521 to 1480 K and include rate coefficients ranging over more than 10 orders of magnitude;[1,6–7,8] the KKS vibrational relaxation and incubation time data cover the temperature range from 542 to 1307 K. Together, these data are almost sufficient to separate the effects of energy transfer and reaction. A combination of steady-state RRKM calculations and time-dependent master equation calculations is used to develop a combined model and show that all of the data are consistent within the model.

In the following sections, we describe the experimental data, calculation methods, RRKM reaction models, and energy transfer models. The success of this modeling approach shows that the conventional view of unimolecular reaction systems is on a solid footing and that the combination of energy transfer data and unimolecular fall-off data can provide stringent tests of RRKM models and thermochemistry. The NB data do not allow an unambiguous identification of

TABLE I. Low-temperature k_∞ measurements:[a] norbornene $\rightarrow c\text{-}C_5H_6 + C_2H_4$.

Reference	log (A_∞/s^{-1})	E_∞ (kcal mol^{-1})	Temperature (K)
6	13.78±0.19	42.75±0.56	577–716
7	13.85	43.47	539–577
8	14.26±0.28	44.54±0.72	521–570
Combined[b]	14.68±0.25	45.53±2.13	521–716

[a]In order to use the Arrhenius expression and reproduce the measured rate coefficients, four digits are reported for A factor and activation energy.
[b]This work: global nonlinear least-squares fit of k_{uni} vs $1/T$, using equal weights for all data points.

the energy transfer collision step size distribution, but we show that three plausible implementations of the exponential model give equally accurate simulations of the data. The choice of energy transfer model affects the deduced reaction critical energy by more than 2 kcal mol^{-1}, however, which shows the importance of energy transfer in determining thermochemistry from unimolecular reaction fall-off data, a factor which has often been neglected.

II. DESCRIPTION OF EXPERIMENTS

A. Low temperature measurements

The thermal unimolecular dissociation of norbornene (bicyclo[2.2.1] hept-2-ene) is a retro-Diels–Alder reaction yielding 1,3-cyclopentadiene and ethylene as stable molecular products

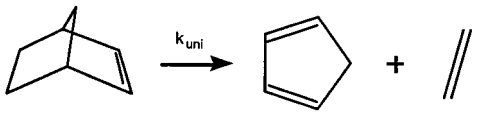

(1)

Prior to the shock-tube study by KKS, unimolecular rate data at low temperatures were obtained by Herndon *et al.*,[6] Roquitte,[7] and Walsh and Wells.[8] All these low temperature data appear to be representative of the unimolecular reaction at its high-pressure limit and the results are consistent with the reaction proceeding via a concerted mechanism.[8,9]

Roquitte[7] studied the decomposition of NB using a conventional static system over the temperature range 539–577 K and pressure range 5–43 Torr. Up to 50% decomposition, the reaction was found to be a clean first-order, homogeneous process (no effect of an increase in surface-to-volume ratio of a factor of 25), unaffected by the free radical chain inhibitors, NO, O_2, propylene, and toluene. At higher percentage decomposition an unidentified third product was detected which, however, was always <2% of the total products. There was no pressure dependence under the experimental conditions. A test for reversibility of the reaction was carried out at 577 K but it proved to be negative. The Arrhenius parameters (error limits were not quoted) were found to be $A_\infty = 10^{13.85}$ s^{-1} and $E_\infty = 43.47$ kcal mol^{-1} (see Table I).

Herndon *et al.*[6] studied the decomposition of NB at about the same time as Roquitte.[7] They used a stirred-flow reactor and a tubular-flow reactor (both at atmospheric pressure) with N_2 as an inert carrier gas over the temperature range 577–671 K (stirred-flow reactor) and 630–716 K (tubular-flow reactor). Again, a first-order homogeneous reaction (the surface-to-volume ratios of the two reactors differed by a factor of 30) producing 1,3-cyclopentadiene and ethylene was confirmed. No other products were detected (upper limit <0.01%), even at the highest temperature investigated. The use of He, CO_2, and steam as alternative carrier gases was found to have no effect on the rate coefficients. The Arrhenius parameters using all data from both reactors were found to be $A_\infty = 10^{13.78\pm0.19}$ s^{-1} and $E_\infty = 42.75\pm0.56$ kcal mol^{-1} where the error limits were stated to be one standard deviation in the least-squares fit (see Table I). Using the data from either reactor alone was found to yield the same Arrhenius parameters within respective error limits.

Walsh and Wells[8] studied both the decomposition of NB and the reverse addition of ethylene to 1,3-cyclopentadiene using a conventional static system. Both kinetic and equilibrium data were obtained. First-order homogeneous kinetics at NB conversions of up to 80% was confirmed and rate coefficients were obtained at six different temperatures over the range 521–570 K. At high conversions (>60%) in a reactor with high surface-to-volume ratio, small quantities (≤3% of NB) of a third product, nortricyclene were observed. The high temperature (<650 K) pyrolysis of the equilibrium mixture of ethylene, 1,3-cyclopentadiene, and NB indicated that no significant homogeneous molecular isomerization of NB occurs with E_∞ less than ~54 kcal mol^{-1}. The decomposition rate coefficients were unaffected by pressure in the range 2–16 Torr. The Arrhenius parameters were found to be $A_\infty = 10^{14.26\pm0.28}$ s^{-1} and $E_\infty = 44.54\pm0.72$ kcal mol^{-1} where the error limits were stated to be one standard deviation (68% confidence level) in the least-squares fit (see Table I).

The Arrhenius parameters from all three low temperature studies are in reasonable agreement. We have carried out a least-squares fit to the combined data of all three studies and find the Arrhenius parameters $A_\infty = 10^{14.68\pm0.25}$ s^{-1} and $E_\infty = 45.53\pm2.13$ kcal mol^{-1} (uncertainties derived in the present work are expressed as one standard deviation). These parameters differ significantly from those of the individual investigations, but the overall fit is satisfactory, if the differences among the investigations reflect the actual experimental errors of each. We cannot identify the cause of the small differences among the individual investigations, but it may be due to both temperature and analytical errors being larger than claimed.

B. Shock-tube experiments and results

KKS studied the thermal decomposition of NB by using the shock-tube laser-schlieren (LS) technique (see Ref. 1 for details). A very wide range of experimental conditions was covered: 542–1480 K in temperature and 34–416 Torr in pressure, using NB/Kr mixtures containing 0.5%, 2%, and 4% NB. The sequence of events which comprise the approach to equilibrium in shock waves can provide at least three distinct energy-transfer related observables.[3,4,10] These are the vibrational relaxation time, τ_{vib}, the incubation time, τ_{inc}, and the steady-state reaction rate coefficient, k_{uni}. KKS were able to obtain measurements of all three parameters. Unimolecular reaction rate data were obtained in the experi-

mental shock-tube regime where reaction alone occurred without vibrational relaxation; this covered the temperature range 869–1480 K and pressure range 43–416 Torr at dilutions of 0.5% and 2% NB in Kr. KKS speculated on the possibility of isomerization of NB, e.g., to 2-methyl-1,3-cyclohexadiene, at the high temperatures of the shock-tube experimental conditions but ruled it out because there was no evidence from the LS density gradient profiles of any reaction other than the decomposition of NB to 1,3-cyclopentadiene and ethylene. In the LS shock-tube experiments, however, product analyses are not carried out and so minor products might have escaped detection.

Unlike the low temperature studies, the reaction is well into the unimolecular fall-off regime under the shock-tube experimental conditions. KKS accounted for unimolecular rate fall-off by using RRKM calculations,[11,12] following the prescription of Gilbert *et al.*[13] To fit the steady-state shock tube data, the RRKM model used by KKS incorporated the reaction threshold or critical energy $E_0=44.2$ kcal mol^{-1}, ''reasonable'' transition-state frequencies, and a constant $\langle\Delta E\rangle_{\text{down}}=280$ cm^{-1} (the average downward energy transferred per collision). KKS noted that $\langle\Delta E\rangle_{\text{down}}$ must be strongly energy-dependent, however, in order to explain the observed relaxation times. They also noted that their data show NB–NB energy transfer collisions to be more effective than NB–Kr collisions. The RRKM extrapolated high-pressure Arrhenius parameters quoted by KKS are $A_\infty=10^{15.02}$ s^{-1} and $E_\infty=46.34\pm0.3$ kcal mol^{-1} over the temperature range 700–1400 K.

The RRKM extrapolation to the high-pressure limit was compared with the results of Herndon *et al.*[6] and Roquitte[7] but KKS overlooked the results of Walsh and Wells.[8] The value for E_∞ obtained from the RRKM model of KKS is clearly in disagreement with the low temperature values obtained by Roquitte and Herndon *et al.* However the value of E_∞ obtained by Walsh and Wells is closer to the KKS value, and the value shown in Table I for the combined low temperature data is closer still. KKS noted that Arrhenius extrapolation of either the Roquitte or the Herndon *et al.* high-pressure limit rate coefficient (k_∞) data to higher temperatures lies on or below the lowest temperature shock-tube data, which are clearly in the fall-off regime. Similarities with the earlier shock-tube LS studies of the retro-Diels–Alder decompositions of 1,2,3,6-tetrahydropyridine[14] and cyclohexene[3] were noted. In these two investigations, extrapolation of reliable low temperature k_∞ data also lies on or below the shock-tube fall-off k_{uni} data. Reconciliation of the KKS data for NB with the two sets of low temperature data would require a small but significant increase in E_∞ with temperature, i.e., a curved Arrhenius plot, while RRKM calculations show very little curvature. KKS made a minimum estimate by joining their RRKM calculated k_∞ at 900 K (5950 s^{-1}) to the highest-temperature rate coefficient of Herndon *et al.* (2.713 s^{-1} at 700 K, calculated from the Herndon *et al.* Arrhenius parameters). The effective E_∞ is thus 48.2 kcal mol^{-1}, which is 5.45 kcal mol^{-1} greater than the Herndon *et al.* value.

KKS argued that an increase in E_∞ of approximately 5 kcal mol^{-1} over the temperature range 600–1100 K is much too large to be accommodated by physically reasonable changes in transition-state frequencies. They proposed that if this increase in E_∞ is real then it reflects a change in reaction mechanism from a low temperature concerted process to a high temperature diradical pathway (O'Neal and Benson[7] estimated a value of 49.1 kcal mol^{-1} for the enthalpy change to form the appropriate diradical from NB). However the effective E_∞ calculated by KKS is only 3.66 kcal mol^{-1} above the Walsh and Wells value and only 2.67 kcal mol^{-1} above the value obtained from fitting the combined low temperature data.

Our analysis of the KKS data, consistent with the energy transfer behavior of the reaction system, shows that it is possible to obtain a reasonable fit of all the low temperature data and the RRKM extrapolation of the shock-tube data to k_∞ with a single set of Arrhenius parameters over the full temperature range of 521–1480 K. Thus it is not necessary to invoke a change in reaction mechanism for high temperature conditions.

III. CALCULATION METHODS

A. Conceptual model and strategy for data fitting

1. The model

Prior to passage of the shock wave, the norbornene vibrational energy is described by a thermal distribution near 300 K. The passage of the shock wave produces a high translational temperature on a very short time scale, due to adiabatic compression. Translations and rotations relax much more rapidly than vibrations,[15] and the NB vibrational (V) temperature remains near 300 K, while its translational/rotational (T/R) temperature comes into equilibrium with the monatomic bath gas within a few collisions. Collisional vibrational activation of the NB now occurs and eventually the NB vibrational energy distribution reaches a steady-state which depends on the translational temperature and the energy-dependent rate of unimolecular reaction.

The vibrational activation process requires many collisions, since the average amount of energy transferred per collision is much smaller than the threshold energy for reaction. As the activation takes place, the vibrational energy distribution is characterized by an increasing average energy and width, as illustrated in Fig. 1. Eventually, a significant fraction of the NB is activated above the reaction threshold and unimolecular reaction occurs. The ''incubation time'' (τ_{inc}) is the delay between the passage of the shock and the onset of unimolecular reaction, as defined in Fig. 2. The ''vibrational relaxation time'' (τ_{vib}) characterizes the transition from the initial to the final vibrational energy distribution. In the absence of unimolecular reaction, the final NB vibrational energy distribution is thermal and at the same temperature as the bath. When unimolecular reaction is significant relative to collisional activation, the final NB steady state vibrational energy distribution is depleted relative to the thermal distribution, resulting in unimolecular reaction rate coefficient fall-off.

The collisional activation of the NB produces a slight reduction of the translational temperature, because $T/R\rightarrow V$ energy transfer converts some translational energy to vibra-

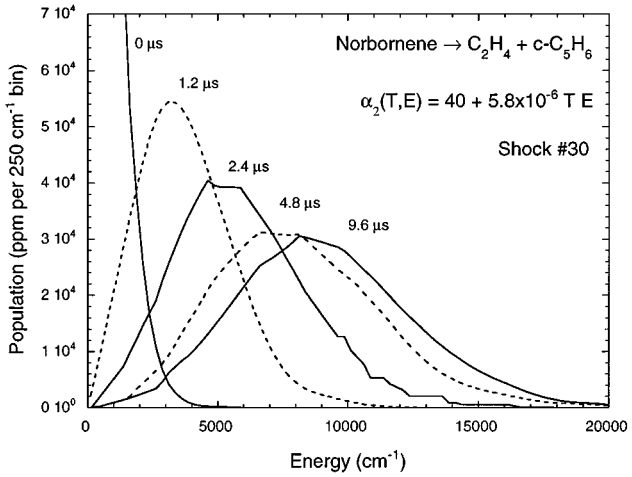

FIG. 1. Evolution of the population distribution (Shock ♯30 from KKS, energy transfer Model 2).

tional energy, while total energy is conserved. The slight temperature decrease produced a density gradient which was observed by KKS in their shock-tube LS experiments. A density gradient also is produced when a unimolecular reaction occurs, because the translational temperature varies as a result of reaction endo- or exothermicity. By monitoring the density gradient as a function of time, KKS observed part of the NB vibrational relaxation and the subsequent onset of unimolecular reaction.

The unimolecular rate coefficients (k_{uni}) determined by KKS for NB decomposition are affected by fall-off, as shown in Fig. 3. In contrast, the lower temperature data obtained in previous studies are near the high pressure limit (k_∞), but the extrapolation of k_∞ to higher temperatures is a long one and is not reliable: RRKM theory is needed for the extrapolation.

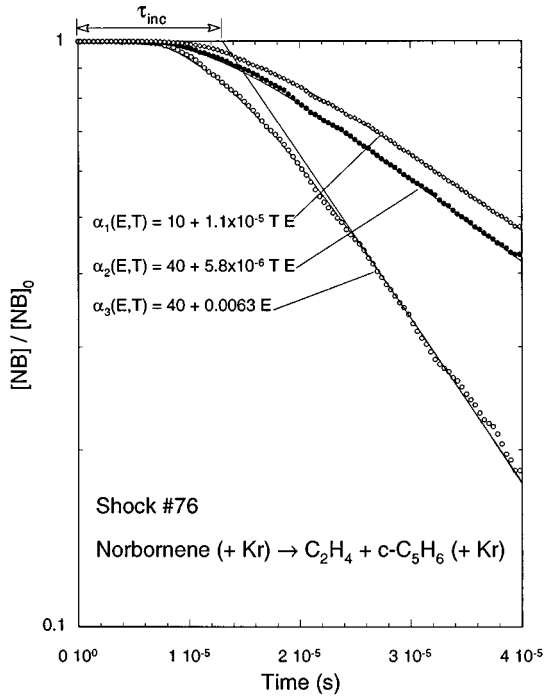

FIG. 2. Incubation and unimolecular reaction in Shock ♯76 (KKS) calculated with three models. The incubation time is shown schematically for Model 3. Least squares fits using Eq. (9) are shown for all three models. The fluctuations are due to the stochastic solution of the master equation.

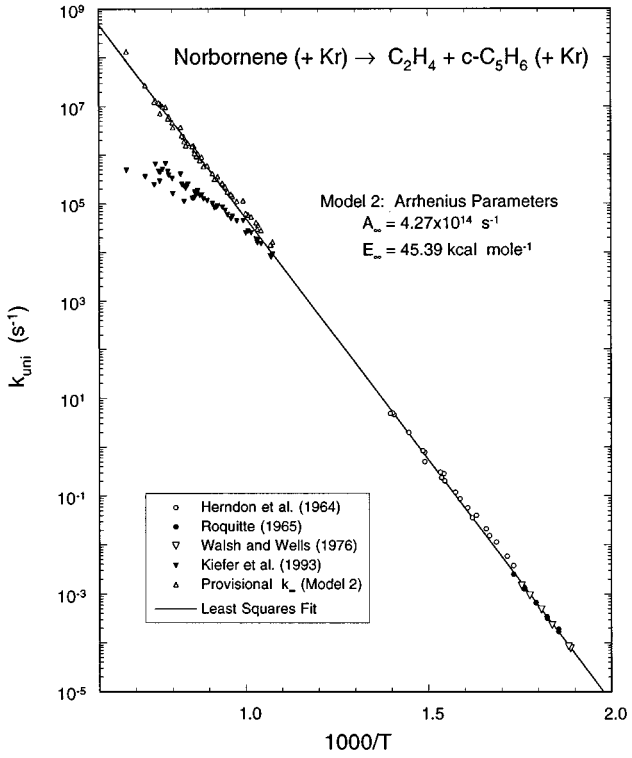

FIG. 3. Arrhenius plot summarizing experimental data and results from Model 2 (the other models show similar good agreement with experiment).

In principle, measured incubation times, vibrational relaxation times, and steady-state unimolecular reaction rate coefficients at each temperature are sufficient to determine the collisional energy transfer parameters at that temperature, as well as the RRKM model for unimolecular reaction. However, experimental uncertainties and the limited temperature and pressure ranges accessible in the experiments significantly limit the uniqueness of the resulting models. Furthermore, the NB vibrational relaxation time and incubation time data are somewhat redundant. We chose to use the incubation times rather than the vibrational relaxation times in the fitting procedure, because we felt the incubation times are better defined experimentally and are therefore more reliable. Furthermore, about 2/3 of the energy relaxation in each experiment was already complete by the time the vibrational relaxation times could be observed, perhaps making the experimental τ_{vib} data less characteristic of the decay; thus we used the τ_{inc} data in the fitting process and then examined the τ_{vib} data as a test for consistency.

To interpret the incubation time data and extract energy transfer parameters, an accurate RRKM model is needed. To find the RRKM model and microcanonical rate coefficients $k(E)$, fall-off corrections must be known, but they can only be deduced if the energy transfer parameters are known. Thus, we used the following assumptions and procedure to arrive at a self-consistent simulation which includes both an

RRKM model for $k(E)$ and energy transfer parameters which are consistent with τ_{inc} and τ_{vib}.

2. Principal assumptions

The time-dependent approach to steady state was simulated by using a detailed time-dependent master equation.[16,17] Several new and noteworthy features of the master equation computer code are described in the Appendix, but the principal assumptions are summarized here.

a. Unimolecular reaction rate coefficients. We used RRKM theory[11–13] to calculate the energy-dependent microcanonical unimolecular rate coefficient $k(E)$. The details of the RRKM model and computer codes are presented below.

b. Collision step size distribution. In order to account for collisional energy transfer, the collision step size (density) distribution $P_c(T,E',E)$ must be incorporated in the master equation.[16,18] The collision step size distribution is the probability that a molecule which initially possessed energy in the range E to $E+dE$ is found in the energy range E' to $E'+dE'$ after a single collision with a bath gas at temperature T. When multiplied by the collision frequency (assumed[19] to be due to collisions between particles which interact according to the Lennard-Jones potential), the collision step size distribution describes the collisional rate of production and loss of population. Unfortunately, $P_c(T,E',E)$ is not known with certainty for any molecule and nothing is known about it for NB. Previous model studies by numerous researchers have shown that the detailed functional form of $P_c(T,E',E)$ makes little difference in single-channel unimolecular reaction rate studies.[11–13] The conventional functional form often arbitrarily chosen for $P_c(T,E',E)$ is the "exponential model"[19,20]

$$P_c(T,E',E)=\frac{1}{N(E)}\exp\left\{\frac{-[E-E']}{\alpha(T,E)}\right\},\quad 0\leqslant E'\leqslant E \tag{2a}$$

$$P_c(T,E',E)=\frac{\rho(E')}{\rho(E)}\frac{N(E)}{N(E')}\exp\left\{-\frac{1}{kT}-\frac{[E'-E]}{\alpha(T,E')}\right\},\quad E\leqslant E'\leqslant\infty, \tag{2b}$$

where $\alpha(T,E)$ is a temperature- and energy-dependent parameter, $\rho(E)$ is the density of states of the molecule at energy E, and $N(E)$ is the normalization constant at energy E. For this model, $\langle\Delta E\rangle_{down}$, the energy transferred in deactivating collisions is given by

$$\langle\Delta E\rangle_{down}=\frac{\int_0^E(E-E')P_c(T,E',E)dE'}{\int_0^E P_c(E',E)dE'}\approx\frac{\alpha-(E-\alpha)\exp(-E/\alpha)}{[1-\exp(-E/\alpha)]}. \tag{3}$$

For E much greater than α, $\langle\Delta E\rangle_{down}\approx\alpha$.

The exponential model has been shown to give good descriptions of data from both unimolecular rate coefficient studies[19,21] and relatively "direct" experiments on energy transfer.[17,22,23] "Supercollisions," in which surprisingly large amounts of energy are transferred per collision,[20,24,25] can be pragmatically and unambiguously defined as any deviation from the exponential model, but the reported deviations are rather small,[17,26,27] even when supercollisions are measurable. Furthermore, it has been shown that the exact details of $P_c(T,E',E)$ are not critically important in single-channel unimolecular reactions. For these reasons and because more complicated models require even larger numbers of undetermined parameters, we adopted the simple exponential model for the present work.

TABLE II. Parameters[a] for $\alpha(E)=c_0+c_1E+c_2E^2$ from IRF experiments at 300 K: krypton collider gas.

Excited species	c_0	c_1	c_2	Reference
Benzene-d_0	28.4	5.21 (−3)	−7.38 (−8)	23,b
Toluene-d_0	36.1	9.85 (−3)	−7.69 (−8)	23,c
Toluene-d_8	49.6	12.9 (−3)	−18.8 (−8)	23,d

[a]Energies expressed in cm^{-1}; 5.21 (−3) denotes 5.21×10^{-3}.
[b]M. L. Yerram, J. D. Brenner, K. D. King, and J. R. Barker, J. Phys. Chem. **94**, 6341 (1990).
[c]B. M. Toselli, J. D. Brenner, M. L. Yerram, W. E. Chin, K. D. King, and J. R. Barker, J. Chem. Phys. **95**, 176 (1991).
[d]B. M. Toselli and J. R. Barker, J. Chem. Phys. **97**, 1809 (1992).

Infrared fluorescence (IRF) experiments[17,23] on energy transfer involving benzene derivatives have shown that the exponential model parameter $\alpha(T,E)$ is approximately proportional to energy at low energies, as summarized in Table II for collisions involving krypton. Based on the IRF experiments, we conclude that $\alpha(T,E)$ is adequately described by a simple linear function of energy for the energy range of importance to norbornene decomposition. At higher energies, most IRF results show a "saturation effect," where $\alpha(T,E)$ tends to become independent of energy. This effect would only affect the NB system at vibrational energies above $\sim$30 000 cm^{-1}, an energy range which is not important at the temperatures of the KKS shock experiments. From Table II, the first and second coefficients vary by about a factor of $\times2$, but the ratio $c_0/c_1=4320\pm983$ cm^{-1} is roughly the same for all three compounds.

The temperature dependence of $\alpha(T,E)$ is not known for the benzene derivatives and the experimental temperature range investigated by KKS is not large enough to allow a reliable determination for NB. Energy transfer experiments using IRF[28] and time-resolved ultraviolet absorption[29] found only a weak temperature dependence for $\alpha(T,E)$, but recent experiments on free radical recombination reactions have found a stronger temperature dependence.[30]

In the present work, we have assumed a relatively flexible functional form for $\alpha(T,E)$

$$\alpha(T,E)=c_0+c_1T^aE. \tag{4}$$

We have considered three models based on Eq. (4). In Model 1, we assumed that $c_0=10$ cm^{-1}, the parameter $a=1$, and c_1 is found by simulating the data. In Model 2, we assumed that $c_0=40$ cm^{-1} (in reasonable agreement with the benzene derivatives), $a=1$, and c_1 was found by simulation. In Model 3, we assumed that $c_0=40$ cm^{-1}, but that there was no temperature dependence ($a=0$), and c_1 was again found by simulation. These choices are arbitrary and many other choices are possible, but we found by simulations that an energy-independent model is *not* consistent with the experi-

mental data, in agreement with KKS. Generally, many energy-dependent models can fit the KKS shock-tube data equally well and the three discussed here are representative and cover a range of physically reasonable assumptions.

3. Data fitting procedure

(1) Assuming the low temperature reaction rate data are at the high-pressure limit, we found a provisional RRKM model by adjusting transition-state frequencies and critical energy (E_0) to obtain agreement with the combined low temperature data.

(2) Using the provisional RRKM model, we determined the energy transfer parameter $\alpha(T,E)$ by comparing the results of trial-and-error simulations with the incubation time data from KKS. [For simplicity, we have ignored the small effects due to NB–NB collisions and have considered all energy transfer to take place by NB–Kr collisions.]

(3) Using $\alpha(T,E)$ from step (2) and the RRKM model from step (1), we used a steady-state RRKM computer code to calculate $(k_{\rm uni}/k_\infty)_{\rm calc}$ for the conditions of each of the shock-tube experiments.

(4) We then used the experimental $k_{\rm uni}$ from KKS and $(k_{\rm uni}/k_\infty)_{\rm calc}$ from step (3) to obtain a "provisional" k'_∞

$$k'_\infty = \frac{k_{\rm uni}}{(k_{\rm uni}/k_\infty)_{\rm calc}}. \tag{5}$$

(5) Combining the low temperature experimental data for k_∞ with the provisional k'_∞ values from step (4), we carried out a least-squares fit and determined a new set of Arrhenius parameters.

(6) We repeated steps (2) to (5) iteratively until we obtained a model which consistently fits both the incubation time data and the experimental $k_{\rm uni}$ data.

The rationale for the data fitting procedure is as follows: for an RRKM model which is only approximately correct, the ratio $(k_{\rm uni}/k_\infty)_{\rm calc}$ is more accurate than the individual calculated values of $k_{\rm uni}$ and k_∞ taken alone and thus the ratio can be used with the experimental $k_{\rm uni}$ to estimate a provisional k'_∞. If the energy transfer parameter $\alpha(T,E)$ is essentially correct, but the RRKM expression for $k(E)$ is overestimated (perhaps due to an underestimate of E_0), $(k_{\rm uni}/k_\infty)_{\rm calc}$ will be underestimated, leading to an overestimate of the provisional k'_∞. When the provisional k'_∞ and low temperature experimental data are considered as a single set of data, the overestimated provisional k'_∞ will lead to a higher estimate of E_0. In the next iteration, the higher E_0 will lead to lower values for k'_∞. The fact that the low temperature data are fitted along with the provisional k'_∞ apparently tends to eliminate oscillations, allowing the process to converge.

We found that the incubation time simulations (carried out using the time-dependent stochastic master equation code,[16] see below) are not very sensitive to large variations (>6 kcal mol^{-1}) in E_0. Thus for each energy transfer model, it was only necessary to search for the proper energy transfer parameters once, as long as a reasonable RRKM model was used. Once suitable parameters for $\alpha(T,E)$ were found, calculations were carried out using the steady-state UNIMOL computer codes[31] (see below) to refine the RRKM vibrational assignment and E_0.

B. RRKM Codes and models

1. Steady-state unimolecular reaction

The shock-tube rate coefficients obtained by KKS for the thermal decomposition of NB were obtained using experimental conditions where the steady-state reaction clearly was in the fall-off regime. RRKM theory can be applied in the usual way to relate these thermal fall-off rate coefficients, $k_{\rm uni}$ to the high-pressure rate coefficients, k_∞. Specifically, RRKM theory is used to calculate the energy-dependent microcanonical rate coefficients, $k(E)$ which then are used to calculate thermal rate coefficients. Several methods are available[12,32] to generate the $k(E)$ but RRKM theory is the most commonly used and is generally recognized to be the most accurate method. The high-pressure limiting k_∞ is obtained by averaging the $k(E)$ over the Boltzmann equilibrium distribution of reactant energy. In the fall-off regime (non-Boltzmann distribution of energy), collisional energy transfer is accounted for in the UNIMOL suite of computer codes[31] by incorporating the $k(E)$ into a steady-state integral eigenvalue master equation

$$\begin{aligned} -k_{\rm uni}g(E) &= \omega\int_0^\infty [P_c(T,E,E')g(E') \\ &\quad - P_c(T,E',E)g(E)]dE' - k(E)g(E) \\ &= [M]\int_0^\infty [R(T,E,E')g(E') \\ &\quad - R(T,E',E)g(E)]dE' - k(E)g(E), \end{aligned} \tag{6}$$

where $R(T,E,E')$ is the rate coefficient for collisional energy transfer from internal energy E' to E, T is the bath-gas temperature, and the eigenfunction $g(E)$ is the steady-state population of molecules with energy E. The collision step size distribution can be written in terms of the rate coefficient for collisional energy transfer

$$P_c(T,E,E') = \frac{[M]R(T,E,E')}{\omega(E')}, \tag{7}$$

where $\omega = k_c[M]$ is the assumed Lennard-Jones collision frequency (commonly assumed to be independent of the initial energy E') corresponding to bimolecular collision rate constant k_c, and $[M]$ is the concentration of bath gas.

The solution to Eq. (6) yields $k_{\rm uni}$ at any pressure. Alternatively, $k_{\rm uni}$ can be found from

$$k_{\rm uni} = \frac{\int_{E_0}^\infty k(E)g(E)dE}{\int_0^\infty g(E)dE}. \tag{8}$$

The solution for $k_{\rm uni}$ from the above equations does not include angular momentum conservation.[11,12,33] This can be included by formulating a microcanonical rate coefficient, $k(E,J)$ which depends on the internal energy and the angular momentum state (J) of a molecule, and formulating energy transfer rate coefficients or probabilities in terms of both E

TABLE III. RRKM model for global simulation of shock-tube and low-temperature data: norbornene→c-C_5H_6+C_2H_4.[a]

Frequencies (cm^{-1}) and degeneracies for the transition state
3091,3105(2),3102,3026,2960,1580,1500(4),1300(2),1126,1202,1123,1060,1032,
997,900(2),940*,320*,435*,590*,395*,3075,2988,3043,2886,1350(2),1206,1294,
1226,1138,950,1006,988,833,664,220*,129*,325*
Frequencies (cm^{-1}) for the molecule[b]
3091,2997,2980,2975,2932,2926,1574,1477,1457,1299,1284,1167,1126,1093,1021,
964,938,906,873,809,769,709,471,381,3063,2991,2959,2916,1455,1339,1285,1270,
1254,1206,1177,1115,1035,950,915,898,833,794,664,494,258
Rotational constants, B (cm^{-1}), and symmetry numbers, σ[c]
(a) Two inactive external rotors in complex, B=0.078 47, σ=1, dimension=2
(b) Two inactive external rotors in molecule, B=0.1071, σ=1, dimension=2
(c) Active rotor in complex, B=0.1457, σ=1
(d) Active rotor in molecule, B=0.1457, σ=1
Other properties
Lennard-Jones collision diameter=0.4592 nm (for NB/Kr pair)[c]
Lennard-Jones potential well depth=240.1 K (for NB/Kr pair)[c]
Molecular mass of NB=94.08 amu
Molecular mass of Kr=83.8 amu
Reaction path degeneracy=1

[a]*denotes adjusted frequencies.
[b]References 1 and 36.
[c]Reference 1.

and J.[33] It is, however, only necessary to include angular momentum conservation when there is a significant change in the rotational energy of the substrate as reactant proceeds to the transition state, as in simple bond–fission reactions (loose transition state with the two fragments separated by large distances). The retro-Diels–Alder elimination of ethylene from NB is a concerted reaction with a tight transition state and the moments of inertia are effectively unchanged. Hence, J conservation is automatically maintained without the necessity of explicitly including rotation effects.[11,12,33]

An appropriate transition-state (TS) model is required for the application of the RRKM theory to generate $k(E)$. Note that if a TS model is adjusted to fit a particular set of values for the Arrhenius parameters, A_∞ and E_∞ at some particular or average temperature within a range, then the degree of fall-off is independent of the exact details of the TS model.[11,12,33] However the details of the TS model determine the temperature dependence, if any, of A_∞ and E_∞. For example, in the case of simple bond–fission reactions with loose transition states, the Gorin TS model gives a distinctly different temperature dependence for A_∞ and E_∞ than does the vibrational model.[12,34] Tight transition states, such as that required for Reaction (1), are generally well fitted using vibrational TS models and generally exhibit only a weak or negligible temperature dependence in A_∞ and E_∞: The Arrhenius plots are nearly straight lines.

The reactant and final TS parameters (critical energy, vibrational frequencies, and rotational constants) used in the RRKM calculations are given in Table III. The vibrational frequencies for NB are the same as those used by KKS, who obtained the frequencies from the experimental observations and *ab initio* calculations reported by Shaw *et al.*[35] Note that the frequency of 1452 cm^{-1} shown in Table V of KKS is a typographical error and should read 1458 cm^{-1}. The external moments of inertia for the molecule (from which were calculated the rotational constants) were also the same as used as by KKS, who took them from the work of Castro *et al.*[36] For the TS, the moments of inertia were as given by KKS and, following their RRKM model, the external rotational degree of freedom that corresponds to the moment of inertia, I_C, was treated as active in both the molecule and the transition state.

The RRKM model of KKS was the starting point for finding an RRKM model consistent with the low temperature k_∞ data. In finding this RRKM model ♯1 and the successive iterations of RRKM models as outlined above, the following NB molecular frequencies were adjusted in the transition state: C–H (sp^2) deformation at 710, bridge deformation at 472, ring deformation (i/p)+ring deformation (o/p) at 381, C–H stretch at 3063, CH_2 wag at 1286, ring deformation (i/p) at 664, ring deformation (o/p) at 495, and ring deformation (o/p) at 258 cm^{-1}, respectively, where i/p is in-plane and o/p is out-of-plane with respect to the six-membered ring part of NB. The C–C stretch at 874 cm^{-1} was taken to be the reaction coordinate.

An energy transfer model is required for the steady-state master equation calculations to obtain k_{uni} at any pressure. However, the pressure dependence of k_{uni} for a single-channel thermal unimolecular reaction is governed primarily by the value of a single moment such as $\langle \Delta E \rangle_{\text{down}}$, rather than the detailed functional form of the energy step size distribution, $P_c(T,E,E')$, although chosen functional forms should be physically realistic.[33] As discussed in Sec. III A above, the commonly used exponential model was chosen for this work, with the expressions for $\alpha(T,E)$ as described.

The calculations were carried out using the RRKM and steady-state master equation programs in the UNIMOL program suite of Gilbert, Smith, and Jordan.[31] This Fortran program package employs RRKM theory and a numerical solution of the master equation. Full details of the calculational procedure may be found in the manual accompanying the UNIMOL package and in the book by Gilbert and Smith.[33] A

limitation of the UNIMOL package is that energy dependent expressions for $\alpha(T,E)$ cannot be used and it was necessary to find average values corresponding to each temperature and pressure. This was accomplished by carrying out steady-state calculations using the stochastic time-dependent master equation code described below. Recent calculations carried out by Knyazev confirm the importance of properly accounting for the energy dependence of the energy transfer parameters in thermal reaction systems.[37]

2. Non-steady-state unimolecular reaction and relaxation

The non-steady-state calculations were performed using a stochastic time-dependent master equation code. Many features of this code have been described previously,[4,16,18] but it has been enhanced in several ways for the present application. Briefly, the master equation is solved by the Gillespie exact stochastic method,[38] which is exact in the limit of an infinite number of stochastic trials. The precision of the calculated result is proportional to $N^{-1/2}$, where N is the number of trials, and the statistical noise is noticeable in the results, for a practical number of trials. The computer time necessary for each trial is nearly proportional to the collision frequency and the simulated time duration. Thus simulations of high pressure reactions at steady state require considerable computer time, which is why we routinely used the UNIMOL codes for steady-state conditions. The relaxation to the final steady state is rapid and the stochastic code was reasonably efficient for the non-steady-state calculations.

Densities and sums of states needed for the RRKM rate coefficients and collision step-size probabilities are calculated by exact counts using the Stein–Rabinovitch[39] version of the Beyer–Swinehart algorithm[40] with a grain size of 25 cm^{-1}. The results of the calculations are ''binned'' as a function of simulated time in various ways for convenience, but the binning does not affect the accuracy of the master equation solution. The code is set up to handle up to three simultaneous parallel unimolecular reaction channels with $k(E)$'s from RRKM theory. Collisional energy transfer obeys detailed balance and microscopic reversibility and virtually any user-defined collision step-size distribution, $P_c(T,E,E')$, can be employed with energy-dependent parameters. In the present work, the exponential model was used with temperature- and energy-dependent $\alpha(T,E)$. Additional features and details of the code are described in the Appendix.

IV. RESULTS AND DISCUSSION

A. Incubation times

The incubation time τ_{inc} refers to the time required to establish a new steady-state following a sudden change in bath temperature. It is manifested by a delay in the onset of unimolecular reaction, as illustrated in Fig. 2, where $\ln\{[A(t)]/[A]_0\}$ is plotted as a function of time after the shock (the shock numbers refer to individual KKS shock experiments; see KKS for details). When steady state is established, the unimolecular reaction is first order with a well-defined rate coefficient k_{uni} and the plot becomes linear. The slope of the straight line in Fig. 2 corresponds to $-k_{\text{uni}}$ and

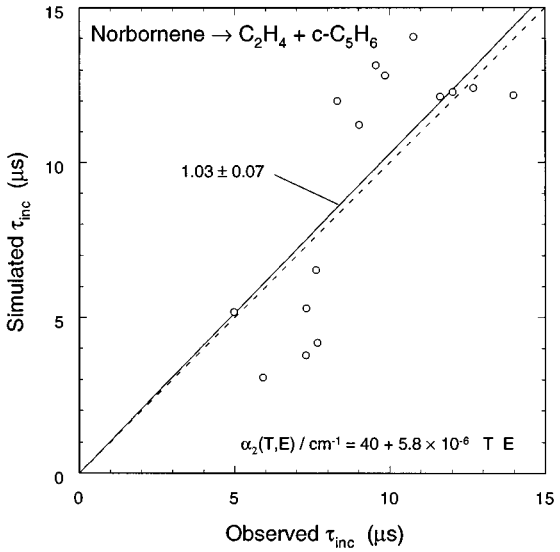

FIG. 4. Comparison of experimental and calculated incubation times for energy transfer Model 2. The broken line shows perfect agreement and the solid line shows actual agreement, according to least squares.

the incubation time is defined as the time when the extrapolated reactant concentration ratio $[A(\tau_{\text{inc}})]/[A]_0=1$, as shown. In the simulations, τ_{inc} was found by least squares fitting with the following empirical function:

$$\frac{[A(t)]}{[A]_0}=\{\exp[-k_{\text{uni}}(t-\tau_{\text{inc}})]\}\{1-\exp[-ct^b]\}. \qquad (9)$$

This empirical function was found to give a reasonable description of the approach to steady state in the simulated experiments and the least squares fit provides values and associated uncertainties for both k_{uni} and τ_{inc}. Because the stochastic solution of the master equation produces statistical ''noise,'' there are uncertainties associated with all of the simulated quantities.

The τ_{inc} values found by the above procedure are in good average agreement with the KKS experimental data, as illustrated in Fig. 4 for energy transfer Model 2. The uncertainties in the individual calculated τ_{inc} values are about the same size as the data symbols in Fig. 4, in most cases. The uncertainties in the experimental data were not stated by KKS, but probably average at least 20%–30% (based on Figs. 5–7 in KKS). The average ratios of calculated to observed τ_{inc} values for the three energy transfer models are 0.95 ± 0.05, 1.03 ± 0.07, and $1.13\pm.08$, which are well within the average uncertainty in the experimental data.

The final results of the fitting process for the three models are as follows:

$$\text{Model 1:}\quad \alpha_1(T,E)=10+1.1\times10^{-5}TE, \qquad (10a)$$

$$\text{Model 2:}\quad \alpha_2(T,E)=40+5.8\times10^{-6}TE, \qquad (10b)$$

$$\text{Model 3:}\quad \alpha_3(T,E)=40+0.0063E, \qquad (10c)$$

where the energies are expressed in cm^{-1}. At 300 K, these equations can be written in the form $\alpha(E)=c_0+c_1E$, where the c_0/c_1 ratios are 3 030, 23 530, and 6 350 cm^{-1}. The first and third values compare favorably with the average ratio of

4320 ± 983 cm^{-1} in Table I, but the value from Model 2 is quite high. The significance of this comparison is uncertain, because of the long temperature extrapolation to 300 K and because it is impossible to determine the true temperature dependence or settle on a preferred energy transfer model on the basis of the NB data.

B. Vibrational relaxation times

In the analysis of shock-tube data, vibrational relaxation is assumed to be driven by the difference in energy between the vibrational energy E and the final steady state energy E_f[41,42]

$$\frac{dE}{dt} = \frac{-1}{\tau_{\text{vib}}}(E - E_f). \tag{11}$$

In general, the phenomenological τ_{vib} is a function of time, because the relaxation involves many energy levels and the vibrational energy is the sum of the level energies, weighted by the level populations. Equation (11) can be integrated to give

$$\int_{E_i}^{E_{\text{vib}}} \frac{dE}{(E - E_f)} = \int_0^t \frac{-dt'}{\tau_{\text{vib}}} = W(t), \tag{12a}$$

$$E_{\text{vib}}(t) = E_f + (E_i - E_f)\exp[-W(t)], \tag{12b}$$

where E_i is the initial vibrational energy at 300 K and E_f is the final steady state vibrational energy. The function $W(t)$ depends on the time dependence of τ_{vib}.

KKS evaluated the vibrational relaxation time from their experimental data by examining the rate of density change $d\rho/dt$ vs time (in the moving-gas frame of reference), where $d\rho/dt$ is proportional to the average vibrational energy remaining to be transferred by the norbornene

$$\frac{d\rho}{dt} \sim (E_f - E_{\text{vib}}). \tag{13}$$

In terms of Eq. (12b) this becomes

$$\frac{d\rho}{dt} \sim (E_f - E_i)\exp[-W(t)]. \tag{14}$$

Plots of experimental $\log(d\rho/dt)$ vs t for norbornene are linear over the accessible time window in the experiments, implying that $W(t)$ is proportional to t and τ_{vib} is independent of time. Uncertainties in τ_{vib} are not stated, but the random scatter in Fig. 11 of KKS indicates an uncertainty of the order of $\pm 20\%$–30%. Furthermore, the experimental time window is limited to the time difference between passage of the shock boundary (t_1) and the time (t_2) when either the reaction becomes significant, or the signal to noise ratio becomes too small. According to KKS, integration of $d\rho/dt$ assuming τ_{vib} is constant gives initial densities ρ_i about 20% greater than the initial densities ρ_0 calculated from thermodynamics. This result supports the conclusion reached by KKS that the experimental τ_{vib} is roughly independent of time, but the initial relaxation rate is somewhat slower than that deduced from τ_{vib} observed in the experimental time window. Thus τ_{vib} is nearly constant, but shows some variation with time.

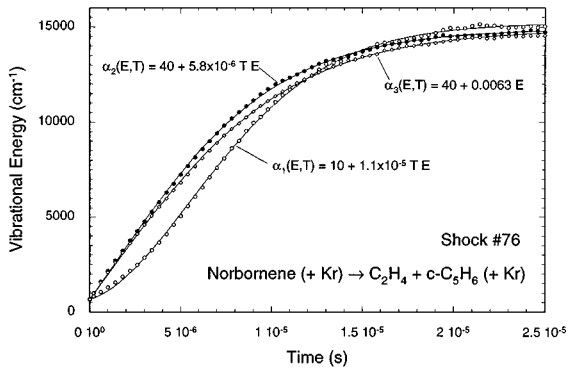

FIG. 5. Relaxation of average energy as calculated with three energy transfer models for Shock ♯76 (KKS). The solid lines show the least squares fits using Eq. (12b) with $W(t) = at + (bt^2)/2$.

In the simulations, E_{vib} was calculated as a function of time and Eq. (12) was used to determine the vibrational relaxation time. Various functions for τ_{vib} were investigated and it was found that the expression $\tau_{\text{vib}} = (a + bt)^{-1}$ provides an excellent description of the phenomenological vibrational relaxation calculated in the simulations. The calculated vibrational energies were fitted to Eq. (12) with $W(t) = at + (bt^2)/2$; E_i, E_f, a, and b were found by nonlinear least squares and the parameters were used to calculate τ_{vib}. An example of the least-squares fit of the energy and the resulting time-dependent τ_{vib} are shown in Figs. 5 and 6, respectively. Since the simulated τ_{vib} depends on time, two methods were used to determine the simulated τ_{vib} appropriate for comparison with experiment. In experiments where the unimolecular reaction becomes important after an incubation time, τ_{vib} was evaluated at $t = \tau_{\text{inc}}$. In experiments

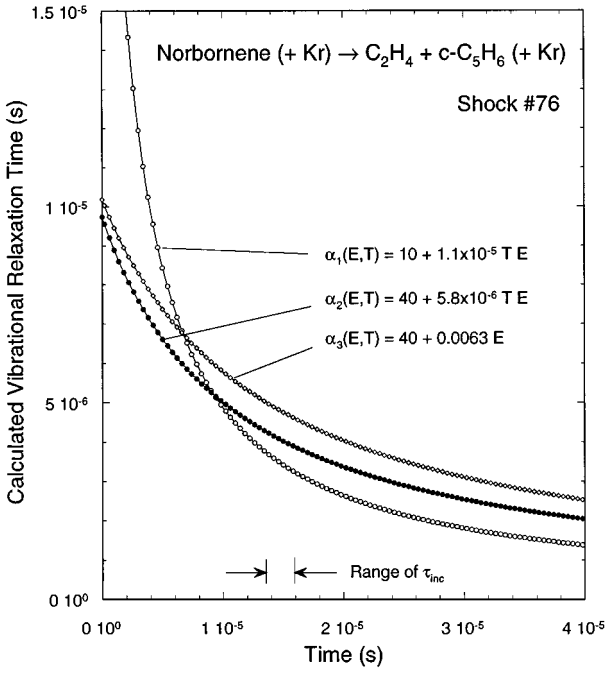

FIG. 6. Vibration relaxation times for three energy transfer models, showing the dependence on time. For the three simulations, the incubation time falls in the range shown.

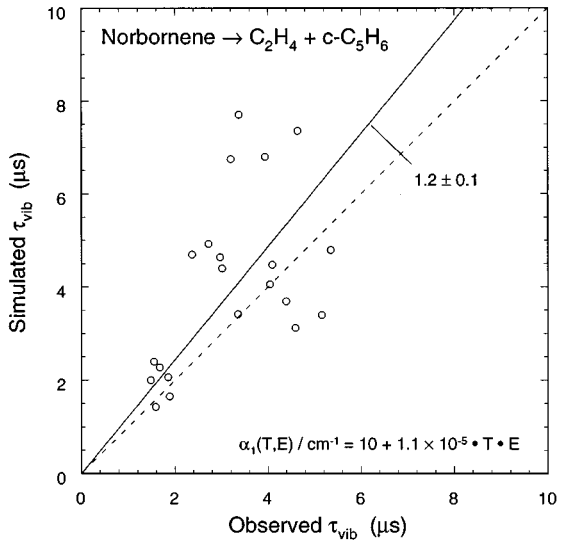

FIG. 7. Comparisons of experimental and calculated vibrational relaxation times (Model 1). The broken line shows perfect agreement and the solid line shows actual agreement, according to least squares.

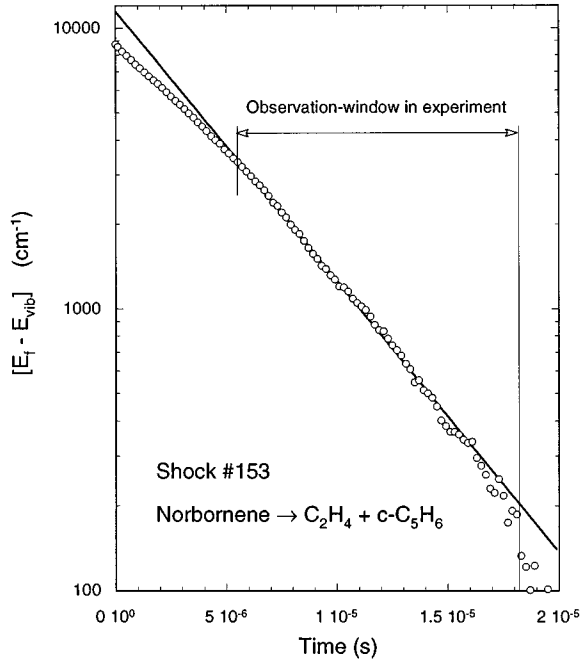

FIG. 8. Vibrational relaxation in Shock ♯153 [see KKS Fig. 3(a)]. Points: simulation; line: exponential least squares fit to data within experimental observation window.

where the unimolecular reaction is not important, τ_{vib} was averaged over the time window of the experiments. This latter procedure was only possible for the six experiments shown in Figs. 2–4 of KKS, where we estimated the time window by scaling the laboratory frame time scale according to the slopes of the plots and the tabulated experimental values of τ_{vib}. Neither of these procedures is completely satisfactory, but the comparison of calculated and experimental τ_{vib} values is used only as a consistency check (for the 15 experiments in Table IV and six experiments in Figs. 2–4 of KKS).

The calculated and experimental τ_{vib} values are compared in Fig. 7 for the 21 simulations. The average ratio of the calculated to the observed values for energy transfer Model 1 is about 1.3 and the least-squares ratio is about 1.2 (maximum and minimum ratios are 2.3 and 0.66); all three models gave essentially similar results. These comparisons show generally good agreement, since the experimental and calculated τ_{vib} values depend differently on time and since they both have uncertainties.

In fact, the only significant difference between the calculations and the experiments is that the calculated τ_{vib} values vary with time, while the experimental values do not. The origin of this difference has not been identified. In the calculations, E_{vib} is calculated directly and its behavior is characterized by the time-dependent τ_{vib}. In the experiments, E_{vib} must be inferred from the time-varying density gradient and is only observed during a relatively brief time window. It was partly because of the complexity in comparing vibrational relaxation times that we chose to use the incubation times as the primary data.

Figure 8 shows the simulated vibrational relaxation corresponding to KKS shock ♯153. During the window of observation, the simulated decay (the points) is almost exponential, but the slight deviation might be detectable in an experiment [compare with KKS Fig. 3(a)]. In the experiments, KKS reported that the ratio of the extrapolated value of the density change to that calculated from thermodynamics (presumed to be accurate) was about 1.4 for this particular shock. The corresponding quantity in the simulations is the ratio of the extrapolated E_f in Figure 8 to the value of E_f actually calculated in the simulations: 1.31, a value in very good agreement with the experiments. The 2% and 4% mixture shocks have an average ratio of about 1.2. KKS concluded from this behavior that τ_{vib} is not exactly constant. The master equation simulations reproduce this tendency.

Since the incubation times and vibrational relaxation times separately show good agreement between simulations and experiments, it is not surprising that their ratio is also in generally good agreement, as shown in Fig. 9 for Model 2

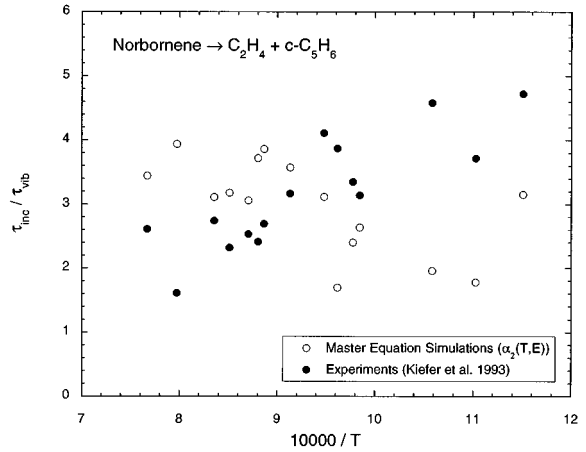

FIG. 9. The $\tau_{\mathrm{inc}}/\tau_{\mathrm{vib}}$ ratio as a function of temperature: experimental and calculated, according to Model 2.

TABLE IV. Energy transfer/RRKM models and results:[a] norbornene→*c*-C_5H_6+C_2H_4 (krypton collider gas).

Exponential model parameter (cm^{-1})	E_0 (kcal mol^{-1})	log (A_∞/s^{-1})	E_∞ (kcal mol^{-1})	Reference
α=280	44.20	15.02	46.34	1
$\alpha_1(T,E)=10+1.1\times10^{-5}$ *TE*	43.66	14.65	45.45	This work
$\alpha_2(T,E)=40+5.8\times10^{-6}$ *TE*	45.80	14.63	45.39	This work
$\alpha_3(T,E)=40+0.0063$ *E*	45.80	14.69	45.56	This work

[a]In order to use the Arrhenius expression and reproduce the measured rate coefficients, four digits are reported for *A* factor and activation energy.

(the other models show similar levels of agreement). The scatter in these data are due, in part, to variations in composition and pressure for the individual shock experiments. The calculations have less than 10% uncertainties, while the experiments are likely uncertain by at least 30%. Except at the lowest temperatures, the calculated results are consistent with the experimental results. The calculated values show no significant variation due to temperature, while the experimental values show a tendency to increase at lower temperatures. The significance of this difference is difficult to evaluate, considering the relatively large uncertainties.

C. Unimolecular rate coefficients and RRKM models

The RRKM model described by the parameters shown in Table III yields the Arrhenius parameters summarized in Table IV for a ''global'' fit encompassing the low temperature k_∞ data and the provisional k'_∞ values calculated from the shock-tube LS $k_{\rm uni}$. These Arrhenius parameters are essentially identical to the values obtained from the least-squares fit to the combined low temperature k_∞ data, and the values for E_0 encompass the value of 44.2 kcal mol^{-1} from the RRKM model of KKS. We found that the RRKM calculations for the NB system using the UNIMOL program suite are not sensitive to variations of $<$0.3 kcal mol^{-1} in E_0, probably because the energy graining in this code is 100 cm^{-1} ($\sim$0.3 kcal mol^{-1}). A ''global'' fit Arrhenius plot is shown in Fig. 3. It is interesting to note that the provisional k'_∞ values show considerably less scatter than the experimental $k_{\rm uni}$ data. This is the result of taking into account the individual pressure of each experimental run when calculating the fall off.

If the final RRKM model alone is used to calculate Arrhenius parameters without the inclusion of the low temperature data then the results are $A_\infty=10^{15.21}$ s^{-1} and E_∞=46.85 kcal mol^{-1} (196 kJ mol^{-1}). These values are slightly higher than the global fit values but well within the uncertainty limits. The slightly higher values obtained by considering the shock-tube data alone probably reflect the effect of the extrema in the data, particularly the rate coefficient at 1480 K and 43 Torr (highest temperature and largest fall-off correction). Note also that these RRKM values for A_∞ and E_∞ are not too different from the values of $A_\infty=10^{15.02}s^{-1}$ and E_∞=46.34 kcal mol^{-1} obtained from the RRKM model of KKS.

It is clear from examination of Fig. 3 that there is no need for an increase in E_∞ over the combined temperature range of the low temperature and shock-tube studies, and hence no need to invoke a shift in reaction mechanism from concerted to diradical for high temperature conditions. The value for E_∞ is $\sim$3.7 kcal mol^{-1} less than the enthalpy change required to form the appropriate diradical.[9]

D. The population distribution and possible future experiments

The end result of these calculations is a model which accurately describes both energy transfer and unimolecular reaction in the NB/Kr nonequilibrium shock-heated system. The model predicts the evolution of the population distribution during and following passage of the shock, as shown in Figs. 1 and 10. Following passage of a shock, the average energy increases smoothly and monotonically until a new steady state distribution is established at the new temperature. The exact details of the energy relaxation depend on the choice of energy transfer model. For example, the energy steps at low total energy are very small for Model 1, in contrast with Models 2 and 3. The small energy steps at the bottom of the energy ladder result in considerable time being spent there and the average energy increases slowly and then accelerates as the energy increases, as shown in Fig. 5. In Models 2 and 3, the step size at the bottom of the ladder is larger than in Model 1, but the step sizes high on the ladder are smaller. Thus the increase in average energy does not show the same degree of acceleration exhibited by Model 1.

The average energy relaxation measurements carried out by KKS are a significant contribution. In addition to the re-

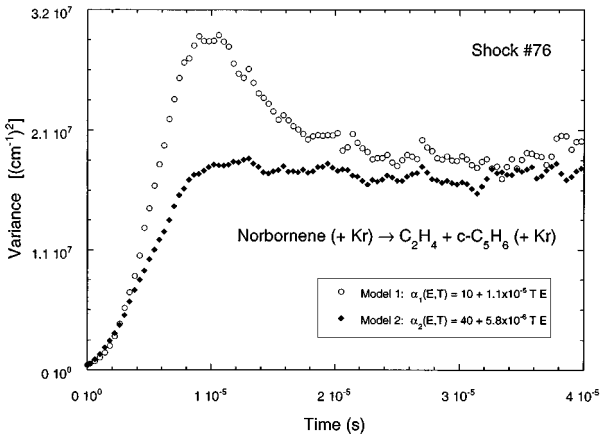

FIG. 10. Calculated population distribution variance for two energy transfer models for KKS Shock ♯76. (The fluctuations are due to the stochastic master equation solution technique.)

laxation of average energy, it would be useful to measure relaxation of the population distribution variance and higher order properties. It is clear in Fig. 1 that the width of the distribution increases along with the average energy. Using information about the higher moments of the population distribution, it would be possible to refine the energy transfer model and determine whether supercollisions are significant. In recent IRF experiments, Brenner and co-workers[17] have shown that higher moments of the distribution can be measured by observing IRF from several infrared emission bands. The same multicolor IRF approach could be used with shock-heated NB. The population distribution variance is closely related to the width of the distribution and it is easily calculated using the stochastic master equation code. Examples for energy transfer Models 1 and 2 are shown in Fig. 10. It is apparent from the figure that measurement of the variance in shock-heated NB could help to identify the favored model.

Other types of experiments can help to determine the temperature dependence and functional form of the energy transfer model. For example, time-resolved IRF and ultraviolet absorbance experiments may prove to be useful, if a suitable method of vibrational excitation can be found. A weakness of these methods is that they rely on photoexcitation followed by radiationless transitions to populate high vibrational levels in the electronic ground state. Another approach would be to carry out overtone transition pumping experiments with NB. By exciting the NB C–H stretch overtones and investigating the pressure and temperature dependence of subsequent decomposition, it may be possible to refine the energy transfer model. When the energy transfer model is identified and is accurately known, the uncertainties in the reaction threshold can be reduced or eliminated.

V. CONCLUSIONS

The main conclusion from the present work is that it is possible to find a unified master equation model with a single reaction channel which can satisfactorily describe all of the energy transfer and unimolecular reaction rate data for NB. It is not necessary to invoke a change in reaction mechanism for high temperature conditions. The TS model is similar to that described by KKS, with only small differences in critical energy and vibrational frequencies.

Three different $\langle \Delta E \rangle_{\text{down}}$ models (based on the exponential step-size distribution) were investigated and each of the three was capable of fitting all of the experimental data. The experimental data are too limited to enable us to identify a preferred model and it was not possible to determine whether the average $\langle \Delta E \rangle_{\text{down}}$ depends on temperature. All three $\langle \Delta E \rangle_{\text{down}}$ models depend linearly on vibrational energy, unlike the KKS model, which assumed that $\langle \Delta E \rangle_{\text{down}}$ is constant. In fact, we found *no* energy-independent $\langle \Delta E \rangle_{\text{down}}$ which can explain the incubation time and vibrational relaxation data while simultaneously fitting the steady-state unimolecular reaction fall-off data. This is the same conclusion reached by KKS. The linear dependence on vibrational energy is consistent with energy transfer data for several benzene derivatives and it is a feature needed in unimolecular reaction computer codes.

An important finding is that the critical energy for reaction, E_0, depends on the assumed $\langle \Delta E \rangle_{\text{down}}$ model. For the three successful models described above, the reaction critical energy varies by slightly more than 2 kcal mol^{-1}, from which we conclude that reaction thermochemistry deduced from unimolecular reaction rate data in the fall-off may vary by a similar amount.

Finally, it should be noted that the measurements of vibrational relaxation time and incubation time are extremely useful in identifying satisfactory energy transfer models for use in the unimolecular reaction fall-off calculations. A satisfactory energy transfer model is especially important for fall-off calculations when the high-pressure limiting rate coefficients are not well known. This is the case for many intermediate and small molecules at high temperatures under shock-tube conditions.

ACKNOWLEDGMENTS

This work was supported by the U.S. Department of Energy, Office of Basic Energy Sciences. We thank Professor J.H. Kiefer for helpful discussions and for kindly supplying details of his experimental results and RRKM calculations. J.R.B. also thanks V. Knyazev for interesting discussions regarding the effects of energy-dependent $\langle \Delta E \rangle_{\text{down}}$ values on thermal rate constants. K.D.K. was supported in part by the USA/Australia Cooperative Science Program.

APPENDIX: STOCHASTIC MASTER EQUATION METHODS

For high vibrational energies, the state densities are very large and the highly excited species may be found with virtually any energy. Assuming a continuum of energies, the master equation consists of the infinite set of coupled differential equations describing the rates of change of the population at every energy. For species $C(t,E)$ at time t and with energy in the range E to $E+dE$, the time rate of concentration change can be written[18,43]

$$\frac{\partial[C(t,E)]}{\partial t} = \int_0^\infty P_c(T,E,E')k_c[M][C(E',t)]dE' - k_c[M][C(t,E)] + \sum_i^{\text{modes}} [C(E+h\nu_i,t)]A_i \times (E+h\nu_i) - \sum_i^{\text{modes}} [C(t,E)]A_i(E) - \sum_m^{\text{channels}} k_m(E)[C(t,E)], \tag{A1}$$

where the normalized collision step-size distribution $P_c(T,E,E')$ is the probability of the collisional transition from energy E' to energy E, k_c is the bimolecular collision rate constant (calculated using Lennard-Jones parameters), $[M]$ is the concentration of colliders, A_i is the effective rate coefficient for spontaneous emission at transition frequency ν_i, and $k_m(E)$ is the rate coefficient for unimolecular reaction according to reaction channel m. The first term describes production of $C(t,E)$ by collisional transitions, the second

term describes collisional deactivation of $C(t,E)$, the third term describes production of $C(t,E)$ by spontaneous emission from higher energy states, the fourth term describes spontaneous emission by $C(t,E)$, and the last term accounts for chemical reactions. When intense electromagnetic fields are present, terms describing absorption and stimulated emission must also be included.

As explained elsewhere,[16] this code employs interpolation of densities of states and other energy-dependent quantities in order to avoid energy graining and to increase computation speed. In the present code, an effort has been made to account for discontinuous and sparse densities of states, which confound interpolation methods based on continuous functions. The approach taken is to use ''double arrays'' for interpolation, in which the first 100 elements correspond to energies from 0 to 2475 cm^{-1}: an energy grain of 25 cm^{-1}. The next 400 elements correspond to energies ranging from 0 to 99 750 cm^{-1} (in 500 cm^{-1} steps) and are also calculated with a 25 cm^{-1} grain. At low energies, where densities of states are sparse, some energy grains may contain no states and reliable interpolation is not possible. At higher energies, where state densities approach a quasicontinuum, interpolation based on continuous functions may be possible, but of uncertain accuracy. Interpolation problems can significantly affect the collisional part of the calculations and here the computer code was enhanced.

Detailed balance is incorporated in the collisional part of the calculation through the use of Eq. (2b). The normalization constants in Eq. (2) are defined as

$$N(E)=\int_0^\infty P_c(T,E',E)dE', \tag{A2}$$

where $P_c(T,E',E)$ is the collision step size distribution and E and E' are the initial and final energies, respectively. In numerical calculations, the integral in Eq. (A2) is truncated at energy E_{top}, which is set high enough for the integral to converge within $\epsilon=10^{-6}$. Since the normalization constant $N(E')$ enters into the expression for $P_c(T,E',E)$ inside the integral, care must be taken in calculating $N(E)$. This was accomplished, as before, in separately evaluating activating and deactivating collisions in an iterative procedure

$$N(E)=\int_0^E P_c(T,E',E)dE'+\int_E^\infty P_c(T,E',E)dE', \tag{A3a}$$

$$N(E)=N_d(E)+N_u(E). \tag{A3b}$$

The normalization $N_d(E)$ for deactivation collisions does not contain $N(E')$ and can be calculated (trapezoid rule) immediately. For activating collisions, $N(E')$ appears in Eq. (2b) and a first estimate is $N(E')\approx N_d(E')$. Using this estimate, a better estimate of $N_u(E)$ is obtained (trapezoid rule), stored, and used in the next iteration. Contributions to the numerical integrals are only considered when states are present within the energy step. It was found that $N(E)$ usually converged to within a few percent after one or two iterations. The probability of an activating step is the ratio $N_u(E)/N(E)$ and this quantity and the normalization factors are stored for use in randomly selecting the step sizes to be used in the stochastic solution of the master equation.

To calculate a randomly selected energy step for a collision, two pseudorandom numbers (uniform random deviates: $0\leqslant R\leqslant 1$) are used, as described elsewhere.[16] The first random number R_1 is compared with the interpolated probability of an activating step in order to select an up or down transition. In either case, numerical integration is used to evaluate the cumulative probability for comparison with random number R_2 and select the magnitude of the step. For example, if $R_1<N_u(E)/N(E)$, then an activation step is selected. For that activating step, the step size is selected by finding the energy X at which the following equality holds:

$$R_2=\frac{1}{N(E)}\int_E^X P_c(T,E',E)dE', \tag{A4}$$

where $N(E)$ is interpolated. This integral is calculated numerically and problems are encountered if it converges slowly, since the interpolation of $N(E)$ is of limited accuracy. In some cases, the numerical integration is carried out until $X\gg E$ and the integral appears to have converged, but it is still less than the interpolated value of $N(E)$. These are cases where the $N(E)$ interpolation is not sufficiently accurate. Under these circumstances, the calculation is repeated, but now using the converged integral in place of $N(E)$. This procedure was found to be essential for accurate results.

These changes to the computer code enable the use of any arbitrary function for the collision step size distribution, regardless of whether an analytical integral exists. Execution of the code is slower than in previous versions, but the accuracy is improved significantly. The steady-state distribution of vibrational energies provides a measure of the accuracy related to the collisional part of the calculation. In previous versions, the calculated thermal distribution function was shifted by several hundred wavenumbers from the correct distribution, but in the present version, virtually no shift is present.

[1] J. H. Kiefer, S. S. Kumaran, and S. Sundaram, J. Chem. Phys. **99**, 3531 (1993).
[2] J. E. Dove, W. S. Nip, and H. Teitelbaum, in *Proceedings of the 15th (International) Symposium on Combustion* (The Combustion Institute, Pittsburgh, 1974), p. 903.
[3] J. H. Kiefer and J. N. Shah, J. Phys. Chem. **91**, 3024 (1987).
[4] J. Shi and J. R. Barker, Int. J. Chem. Kinet. **22**, 187 (1990).
[5] R. J. Malins and D. C. Tardy, Int. J. Chem. Kinet. **9**, 1007 (1979).
[6] W. C. Herndon, W. B. Cooper, and M. J. Chambers, J. Phys. Chem. **68**, 2016 (1964).
[7] B. C. Roquitte, J. Phys. Chem. **69**, 1351 (1965).
[8] R. Walsh and J. M. Wells, J. Chem. Soc., Perkin Trans. 2 **52** (1976).
[9] H. E. O'Neal and S. W. Benson, Natl. Stand. Ref. Data Ser., Natl. Bur. Stand. No. 21 (1970), p. 336.
[10] J. E. Dove and J. Troe, Chem. Phys. **35**, 1 (1976).
[11] P. J. Robinson and K. A. Holbrook, *Unimolecular Reactions* (Wiley, London, 1972).
[12] W. Forst, *Theory of Unimolecular Reactions* (Academic, New York, 1973).
[13] R. G. Gilbert, K. Luther, and J. Troe, Ber. Bunsenges. Phys. Chem. **87**, 169 (1983).
[14] S. S. Sidhu, J. H. Kiefer, A. Lifshitz, C. Tamburu, J. A. Walker, and W. Tsang, Int. J. Chem. Kinet. **23**, 215, (1991).
[15] J. T. Yardley, *Introduction to Molecular Energy Transfer* (Academic, New York, 1980).

[16] J. R. Barker, Chem. Phys. **77**, 201 (1983).
[17] J. R. Barker, J. Phys. Chem. **96**, 7361 (1992).
[18] J. D. Brenner, J. P. Erinjeri, and J. R. Barker, Chem. Phys. **175**, 99 (1993).
[19] D. C. Tardy and B. S. Rabinovitch, Chem. Rev. **77**, 369 (1977).
[20] I. Oref and D. C. Tardy, Chem. Rev. **90**, 1407 (1990).
[21] M. Quack and J. Troe, in *Gas Kinetics and Energy Transfer*, Vol. 3, edited by P. G. Ashmore and R. J. Donovan, Specialist Periodical Reports (The Chemical Society, London, 1977), p. 175.
[22] H. Hippler and J. Troe, in *Bimolecular Collisions*, edited by J. E. Baggott and M. N. Ashfold (London, The Royal Society of Chemistry, 1989), p. 209.
[23] J. R. Barker and B. M. Toselli, Int. Rev. Phys. Chem. **12**, 305 (1993).
[24] S. Hassoon, I. Oref, and C. Steel, J. Chem. Phys. **89**, 1743 (1988).
[25] I. M. Morgulis, S. S. Sapers, C. Steel, and I. Oref, J. Chem. Phys. **90**, 923 (1989).
[26] H. G. Lohmannsroben and K. Luther, Chem. Phys. Lett. **144**, 473 (1988).
[27] K. Luther and K. Reihs, Ber. Bunsenges. Phys. Chem. **92**, 442 (1988).
[28] J. R. Barker and R. Golden, J. Phys. Chem. **88**, 1012 (1984).
[29] M. Heymann, H. Hippler, and J. Troe, J. Chem. Phys. **80**, 1853 (1984).
[30] For example, see Y. Feng, J. T. Niiranen, A. Benscura, V. D. Knyazev, D. Gutman, and W. Tsang, J. Phys. Chem. **97**, 971 (1993), and references therein.
[31] R. G. Gilbert, S. C. Smith, and M. J. T. Jordan, *UNIMOL program suite (calculation of fall-off curves for unimolecular and recombination reactions)*, 1993. Available from the authors: School of Chemistry, Sydney University, NSW 2006, Australia.
[32] R. E. Weston, Int. J. Chem. Kinet. **18**, 1259 (1986).
[33] R. G. Gilbert and S. C. Smith, *Theory of Unimolecular and Recombination Reactions* (Blackwell Scientific, Oxford, 1990).
[34] S. W. Benson, Can. J. Chem. **61**, 881, (1983).
[35] R. A. Shaw, C. Castro, R. Dutler, A. Rauk, and H. Wieser, J. Chem. Phys. **89**, 716 (1988).
[36] C. R. Castro, R. Dutler, A. Rauk, and H. Wieser, J. Mol. Struct. (Theochem) **152**, 241 (1987).
[37] V. Knyazev, (private communication, 1995).
[38] (a) D. T. Gillespie, J. Comput. Phys. 22, 403 (1976); (b) J. Phys. **81**, 2340 (1977); (c) J. Comput. Phys. **28**, 395 (1978).
[39] S. E. Stein and B. S. Rabinovitch, J. Chem. Phys. **58**, 2438 (1973).
[40] T. Beyer and D. F. Swinehart, Comm. Assoc. Comput. Machines **16**, 379 (1973).
[41] N. H. Johannsen, J. Fluid Mech. **10**, 25 (1961).
[42] P. A. Blythe, J. Fluid Mech. **10**, 33 (1961).
[43] J. R. Barker, J. D. Brenner, and B. M. Toselli, in *Vibrational Energy Transfer Involving Large and Small Molecules*, edited by J. R. Barker Adv. Chem. Kinetics and Dyn., Vol. 2 (in press).